Доклади на Българската академия на науките
Comptes rendus de l'Académie bulgare des Sciences
Tome 78, No 7, 2025

PHYSICS
Photonics

TUNING THE GOUY PHASE OF LASER BEAMS BY NECKLACE-LIKE STRUCTURES OF OPTICAL VORTICES

Nasko Gorunski[1], Maria Mincheva[1], Edmon Lazarov[1], Ivan Stefanov[1], Aleksander Stefanov[2,3], Lyubomir Stoyanov[1], Alexander Dreischuh[1,4,5]✉

Received on May 1, 2025
Accepted on May 27, 2025

Abstract

In this work, we report numerical simulations and experimental results indicating the possibility of determining and controlling the rate of change of the Gouy phase of structured Gaussian-like beams. This is achieved by nesting singly-charged optical vortices with the same signs of their topological charges in necklace-like structures.

Key words: Gouy phase, optical vortex, structured beam

1. Introduction. Any focused Gaussian laser beam experiences an axial phase shift with respect to a reference plane wave when passing through its focus. This phase shift $\Phi_G = \arctan(z/L_D)$ is named after Gouy – the first scientist who investigated it. Here L_D and z are the Rayleigh diffraction length and the longitudinal coordinate, respectively. First studied in the microwave and laser

We gratefuly acknowledge funding of the Bulgarian National Science Fund (project KP-06-H78/6). This work was also supported by the Bulgarian Ministry of Education and Science as a part of the National Roadmap for Research Infrastructure, project ELI ERIC BG and by the European Regional Development Fund under "Research Innovation and Digitization for Smart Transformation" programme 2021–2027 under Project BG16RFPR002-1.014-0006 "National Centre of Excellence Mechatronics and Clean Technologies". N.G., L.S. and A.D. were also supported by the European Union NextGenerationEU through the "National Recovery and Resilience Plan of the Republic of Bulgaria, project BG-RRP-2.004-0008-C01". L.S. would like to gratefully acknowledge the Return Grant awarded by the Alexander von Humboldt Foundation.
https://doi.org/10.7546/CRABS.2025.07.03

beam optics (see e.g. [1–3]), the Gouy phase appears to be important in many other fields as well, e.g. in nonlinear optics [4]. The reason is that the n-th order nonlinear polarization is experiencing a phase shift that is n times larger than that experienced by the fundamental pump wave [2, 3]. Hence, the Gouy phase is expected to have profound consequences in highly nonlinear processes like above-threshold ionization [3] and high-harmonic generation [5].

For higher-order Laguerre–Gaussian (LG) modes with mode indices (m, p) the Gouy phase of the Gaussian beam $\Phi_G = \arctan(z/L_D)$ is multiplied by a factor of $(1 + |m| + 2p)$ [6, 7]. Here, $|m|$ accounts for the fact that the azimuthal mode index m (positive or negative integer number) represents the on-axis topological charge (TC) of the point-phase dislocation carried by optical vortices (OVs). The factor $2p$ is related to the radial mode index p of the LG beam. Very similar is the situation with the Hermite–Gaussian (HG) beams, where their Gouy phases are also multiplied by a factor related to the mode indices, in this case $(1+l+m)$ [8]. Of particular interest (especially in nonlinear optics) is the possibility to control the Gouy phase while preserving the clearly pronounced and dominant central peak of the laser beam. Obviously, this could not be achieved with HG modes. In principle, one could rely on the formation of radial rings of the LG modes at radial mode number $p > 0$, provided that the on-axis vortices are excluded, because at their cores the intensity drops down to zero. In this paper, however, we use another approach.

In essence, the proposed idea is based on singular optics achieved through proper laser beam structuring. It is known that a pair of vortices with identical topological charges, which are formed to be symmetrically offset from the axis of the background laser beam, interact by repelling each other (if they are close enough) and rotating around the axis of the background beam when propagating [9, 10]. This rotation should affect the Gouy phase, which is defined along the beams' axis. The number of optical vortices with identical TCs and the radius of the necklace-like ring within which they are arranged are two possible control parameters for the Gouy phase. However, many OVs arranged within a ring of small radius would strongly repel each other and probably will have less influence on the Gouy phase.

In this work, we report numerical simulations and experimental data indicating the possibility to control the Gouy phase, and particularly its rate of change, by necklace-like structures of singly-charged OVs with the same signs of the TCs. The presented interferometric measurements with OV rings of up to 6 OVs are in good qualitative agreement with the numerical data.

2. Numerical procedure and initial conditions. To numerically simulate the two-dimensional diffraction of the beams of interest, we numerically solved the linear paraxial equation for the slowly-varying optical beam envelope amplitude E

$$ik(\partial E/\partial z) + (1/2)(\partial^2/\partial x^2 + \partial^2/\partial y^2)E = 0, \tag{1}$$

where k is the wave number, (x, y) are the transverse Cartesian coordinates, and z is the longitudinal coordinate. In this analysis, the computational windows are spanned over 1024×1024 grid points. As input unperturbed background beams, we used Gaussian beams with a form-factor $\exp(-r^2/\omega_0^2)$. In this manuscript, the width of the Gaussian beam in the beam waist, assumed at $z = 0$, is kept $\omega_0 = 0.28$ arb. units and $(x, y) \in [-5.11, 5.12]$. The test numerical data obtained using Eq. (1) are in excellent agreement with the known theoretical result for a pure Gaussian beam ($\Phi_G = \arctan(z/L_D)$ with $L_D = 6.6$ arb. units; [11]). With this scaling of the Gaussian beam size at its waist, the intensity and phase distributions of the beam were followed with good accuracy up to the reasonably large distances $z > 9L_D$. As a second step in the tests, we calculated the Gouy phase for Laguerre–Gaussian beams with zero radial mode index ($p = 0$) for azimuthal mode indices $m = 1, 3, 6$, and 9 (i.e. for OVs with different TCs). The resulting numerical data for the different TCs m perfectly followed the theoretical relationship $\Phi_G = (1 + |m| + 2p) \arctan(z/L_D)$ up to $z = 9L_D$ for $m = 1$, up to $z = 7L_D$ for $m = 3$, up to $z = 3.5L_D$ for $m = 6$, and up to $z = 2L_D$ for $m = 9$. The above is valid for generating these LG beams from both initial amplitude and phase modulation as well as for generating them from initial phase modulation only. At the maximum propagation lengths for each of the mentioned cases, the difference between the computed Gouy phases was always smaller or of the order of 10^{-8} rad.

The first attempt to find a way to control the Gouy phase was focused on the coaxial superposition of a Laguerre–Gaussian vortex beam and a Gaussian beam (see Eq. (19) in [12]). Assuming that the waist of each of the analyzed beams is located at $z = 0$, the coaxial superpositions [12] can be rewritten in the form

$$Re[E(r, \varphi, z = 0)] = \exp(-r^2/\omega_0^2)[r^m \cos(m\varphi) - r_0^m], \tag{2a}$$

$$Im[E(r, \varphi, z = 0)] = \exp(-r^2/\omega_0^2) r^m \sin(m\varphi), \tag{2b}$$

$$\Phi(r, \varphi, z = 0) = \arctan\left\{\frac{r^m \sin(m\varphi)}{r^m \cos(m\varphi) - r_0^m}\right\}, \tag{3}$$

in which the relationship between the Cartesian and cylindrical coordinates (x, y) and (r, φ) is the usual one. Here, m is the number of optical vortices with unit topological charges located like a necklace along an imaginary circle of radius r_0 in the wings of the Gaussian beam. The extensive numerical simulations of the evolution of coherent superpositions of a Laguerre–Gaussian vortex beam and a Gaussian beam at $r_0/\omega_0 = 0.8, 0.9, 1.0, 1.1, \ldots, 1.9, 2.0$ and $m = 1, 2, \ldots, 12$ showed the same result: Regardless of r_0/ω_0 and m, the Gouy phase always remains that of the fundamental Gaussian beam $\Phi_G = \arctan(z/L_D)$. (This is proved analytically, based on Eqs. (2) and (3), but we will refrain from presenting

this proof here.) The reason is that the above formulas describe the so-called r-vortices, the radii of the cores of which are related to the width of the background beam carrying them. In order to decouple this dependence, we decided to further generate the desired necklace-like structures composed of OVs using only an initial phase modulation described by the compact expression for their phases given by Eq. (3).

3. Results. As an example, grayscale panels (a) and (b) in Fig. 1 visualize the phase distributions used to generate structured beams with 3 and 6 OVs arranged in a ring (see panels (c) and (d) in the same figure). The graph in Fig. 1 indicates the possibility of controlling the rate of change of the Gouy phase of laser beams with dominant central peaks by controlling the number m of optical vortices arranged in a necklace-like structure. The reference curve is that of the pure Gaussian beam (with no OVs embedded in it), represented by a dashed curve and denoted by the symbol 'G'. For better visibility of the data, the propagation length of each of the beams is shown up to $2L_D$. Transient oscillations are seen in the Gouy phase at the beginning of the propagation of the beams, up to about $0.1L_D$, after which the curves stabilize and become monotonically increasing. These oscillations are due to the use of an initial phase modulation only, causing later the corresponding amplitude/intensity modulation of the beam (see Fig. 3 in [13]). For all curves the asymptotic value of the Gouy phase is $\pi/2$ (not shown on the graph). The important key result is the different rates of change (increase) of the Gouy phase. This is observed in the fan-like spread of curves corresponding to different numbers of optical vortices m carried by the background Gaussian beam. The specific numerical data correspond to a relatively narrow vortex ring as compared to the size of the Gaussian beam ($r_0/\omega_0 = 0.8$).

The 3-D plot in the right part of Fig. 1 is an attempt to summarize the numerical results. It shows that at the same fixed propagation length ($z = 1L_D$ in this case) and for the same background Gaussian beam, the Gouy phase increases with increasing both the number m of OVs in the necklace-like structure and with decreasing the radius of the vortex ring r_0. As in the graph in the middle, the Gouy phase is presented in units of $\pi/2$.

To experimentally measure the Gouy phase of laser beams carrying necklace-like structures of optical vortices, we used a setup based on a single-lens interferometer [14, 15] and a phase-only spatial light modulator. Briefly, a lens without antireflection coating (here, with a focal length $f = 1.5$ m), after two weak Fresnel reflections from its surfaces, forms a secondary beam. It is focused at a much shorter distance f_{eff} than the focal length f of the lens itself ($f_{\mathit{eff}} = f(n-1)/(3n-1) \approx 21.4$ cm; n – refractive index of the glass). This secondary beam is co-axial with respect to the "primary" beam, thus serving as a reference beam in the single-lens interferometer. A clear interference pattern between these two beams can be observed in a short range of distances (≈ 7 cm in this experiment). Within the range of the visibility of the interference pattern,

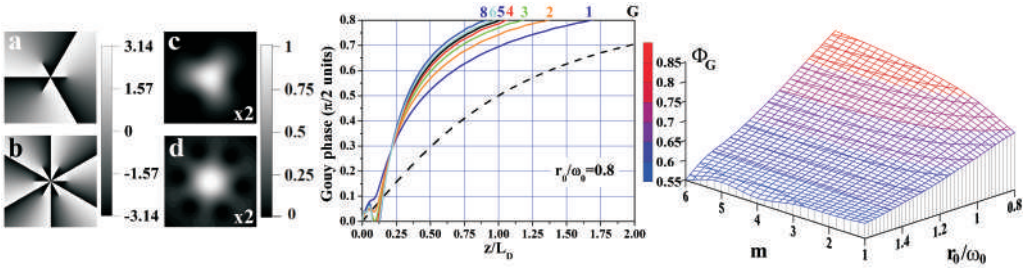

Fig. 1. Numerical results. Panels (a) and (b): Greyscale images of the phase distributions used to generate beams with 3 and 6 OVs arranged in a ring. Panels (c) and (d): Corresponding intensity distributions, magnified by a factor of 2 for better visibility. Graph: Calculated Gouy phase Φ_G (in $\pi/2$ units) vs. beam propagation length z (in units of Rayleigh diffraction length L_D of the Gaussian background beam) for different numbers of OVs (see the notations above the graph) ordered in a necklace-like structure with $r_0/\omega_0 = 0.8$. The initial Gaussian beam width is kept $\omega_0 = 0.28$ arb. units. The data for the pure Gaussian beam are presented with dashed curve and are labelled with 'G'. 3-D plot: Compact representation of the numerical results: Calculated Gouy phase Φ_G (in units of $\pi/2$) at propagation length $z/L_D = 1$, as a function of the normalized radius of the OV ring r_0/ω_0 and the number m of these vortices

the weakly converging "primary" beam is only slightly reshaped. Charge-coupled device (CCD) camera placed on a rail was translated along the beam propagation axis within this region of visibility. At each position, the CCD camera captured an interferogram. In panels (a) and (b) in Fig. 2 we show two interference patterns recorded symmetrically on the two sides of the focus of the secondary beam. The positions of each of the 6 OVs composing the necklace-like beam can be identified by the splittings of one interference ring into two. The opposite directions of the spirals (and the splittings) on the two frames are due to the inversion of the TCs of the OVs around the secondary beam waist. The accumulation of a Gouy phase can be clearly recognized by the dark beam centre in Fig. 1(a) and the brighter beam centre in Fig. 1(b). From each interferogram recorded at different position we extracted the intensity in the beam centre. We will denote this signal as an axial interference signal. One such measurement obtained with 6 OVs surrounding the beam is presented in Fig. 2(c) with hollow circles. The red solid curve approximates this axial interference signal with a function of the type:

$$(4)\quad f(z) = A + B(z-C) + D/\{1+[(z-E)/F]^2\}^{1/2}\cos\{\arctan[(z-G)/H]+I\},$$

where z is the longitudinal coordinate. The second term involving parameters B and C accounts for the weak longitudinal intensity variation of the background beam around the beam waist of the secondary beam. D, E and F account for the intensity variation of the secondary beam itself. Parameters G and H are related to the Gouy phase, while I is an adjustable phase shift. The open circles in Fig. 2(d) show the Gouy phase deduced from the experimental data, whereas the phase calculated from the fit function is shown with a red solid curve.

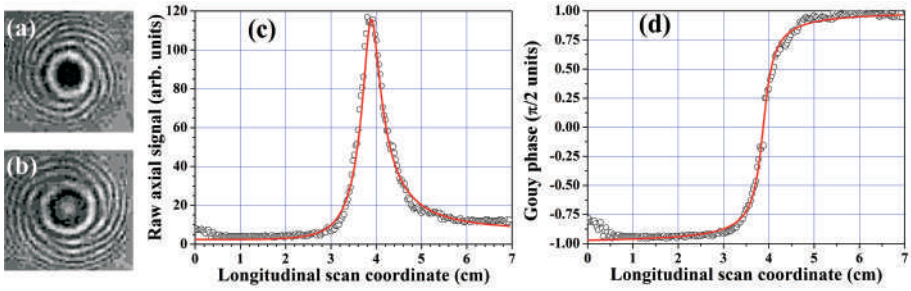

Fig. 2. Six OVs arranged in a necklace-like structure. (a) and (b) – interference patterns recorded symmetrically on the two sides of the focus of the secondary beam (at 2 cm and at 6 cm); (c) – Axial interference signal (hollow circles) between the primary and the secondary beam for $r_0/\omega_0 = 1.2$. Solid curve – approximation of the normalized interference signal (see Eq. 4 and the text for details). (d) – Gouy phase retrieved from the experimental data (open circles) and calculated from the fit function (red solid curve)

Figure 3 shows a comparison between the Gouy phase for an unperturbed Gaussian beam (solid curve) and beams carrying necklace-like ring structures with 3 and 6 optical vortices. The hollow circles represent the experimental data, the solid curves – the respective approximations based on Eq. (4). The beam waists are always located at $z = 0$, where the Gouy phase is crossing the zeroth level.

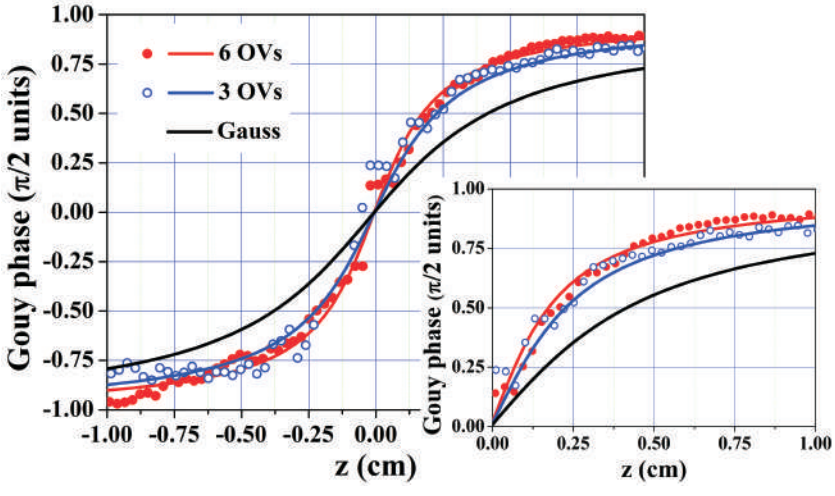

Fig. 3. Longitudinal change of the Gouy phase around the secondary beam focus ($z = 0$) for a non-perturbed Gaussian beam and for those carrying necklace-like structures with 3 and 6 OVs. Hollow circles – experimental data. Solid curves – data extracted from the corresponding interpolation curves. For better visualization, the experimental data for the Gaussian beam is not shown here. Inset: Magnified upper right quarter of the main graph for better visualization

Under this assumption, it is clearly seen that for negative offsets from the beam waist:
— the Gouy phase Φ_G of the Gaussian beam is the least deviated from the zero value,
— for a necklace-like structure with 3 OVs Φ_G is more deviated, and
— for 6 OVs the Gouy phase has the largest (negative) deviation.
Conversely, for positive offsets from the secondary beam focus, the Gouy phase increases the slowest for the Gaussian beam and more strongly for the beams carrying rings with more optical vortices. For clarity, the inserted graph in Fig. 3 is enlarged and shows one quarter of the main graph. It further illustrates the ability to control the Gouy phase growth rate in beams featuring a distinct central peak and vortex necklace-like structures.

4. Conclusion. In view of the numerical and experimental results discussed above, we conclude that the longitudinal rate of change of the Gouy phase Φ_G of beams with well pronounced and dominating axial peaks can be controllably increased at least by a factor of 2. This can be easily achieved by intentionally creating ring-like structures of optical vortices with unit topological charges in the wings of the background (Gaussian) beams. In our view, the presented results form a reasonable basis for the optimization of the controllability of Φ_G either by the radius of the vortex necklace structure or by the number of the optical vortices created by phase modulation only, or even by both approaches.

REFERENCES

[1] Feng S., H. G. Winful (2001) Physical origin of the Gouy phase shift, Opt. Lett., **26**(8), 485–487, https://doi.org/10.1364/OL.26.000485.

[2] Boyd R. W. (2008) Nonlinear Optics (3rd ed.), Academic Press, ISBN 978-0-12-369470-6.

[3] Lastzka N., R. Schnabel (2007) The Gouy phase shift in nonlinear interactions of waves, Opt. Express, **15**(12), 7211–7217.

[4] Lindner F., G. G. Paulus, H. Walther et al. (2004) Gouy phase shift for few-cycle laser pulses, Phys. Rev. Lett., **92**(11), 113001, https://doi.org/10.1103/PhysRevLett.92.113001.

[5] Ghomashi B., R. Reiff, A. Becker (2021) Coherence in macroscopic high harmonic generation for spatial focal phase distributions of monochromatic and broadband Gaussian laser pulses, Opt. Express, **29**(24), 40146–40160, https://doi.org/10.1364/OE.444317.

[6] Hamazaki J., Y. Mineta, K. Oka, R. Morita (2006) Direct observation of Gouy phase shift in a propagating optical vortex, Opt. Express, **14**(18), 8382–8392, https://doi.org/10.1364/oe.14.008382.

[7] He J., X. Wang, D. Hu et al. (2013) Generation and evolution of the terahertz vortex beam, Opt. Express, **21**(17), 20230–20239, https://doi.org/0.1364/OE.21.020230.

[8] Stoyanov L., N. Gorunski, M. Mincheva et al. (2024) Experimental verification of the Gouy phase for higher-order Hermite–Gaussian beams, C. R. Acad. Bulg. Sci., **77**(8), 1138–1145..
[9] Rozas D., C. T. Law, G. A. Swartzlander Jr. (1997) Propagation dynamics of optical vortices, J. Opt. Soc. Am. B, **14**(11), 3054–3065.
[10] Stoyanov L., N. Gorunski, M. Zhekova et al. (2019) Vortex interactions revisited: Formation of stable elementary cells for creation of rigid vortex lattices, Proc. of SPIE **11047**, 110471D, https://doi.org/10.1117/12.2516531.
[11] Linfoot E. H., E. Wolf (1956) Phase distribution near focus in an aberration-free diffraction image, Proc. Phys. Soc. London, Sect. B, **69**(8), 823–832, https://doi.org/10.1088/0370-1301/69/8/307.
[12] Kovalev A. A., V. V. Kotlyar, A. G. Nalimov (2021) Topological charge and asymptotic phase invariants of vortex laser beams, Photonics, **8**(10), 445, https://doi.org/10.3390/photonics8100445.
[13] Stoyanov L., G. Maleshkov, M. Zhekova et al. (2018) Far-field pattern formation by manipulating the topological charges of square-shaped optical vortex lattices, J. Opt. Soc. Am. B, **35**(2), 402–409, https://doi.org/10.1364/JOSAB.35.000402.
[14] Peatross J., M. V. Pack (2001) Visual introduction to Gaussian beams using a single lens as an interferometer, Am. J. Phys., **69**(11), 1169–1172.
[15] Munjal P., K. P. Singh (2019) A single-lens universal interferometer: Towards a class of frugal optical devices, Appl. Phys. Lett., **115**(11), 111102, https://doi.org/10.1063/1.5108587.

[1]*Department of Quantum Electronics, Faculty of Physics,*
Sofia University "St. Kliment Ohridski", 5 J. Bourchier Blvd, 1164 Sofia, Bulgaria
e-mails: naskog@phys.uni-sofia.bg, mariatm@uni-sofia.bg,
eelazarov@uni-sofia.bg, lambrev@phys.uni-sofia.bg,
l.stoyanov@phys.uni-sofia.bg, ald@phys.uni-sofia.bg

[2]*Department of Mechatronics, Robotics and Mechanics,*
Faculty of Mathematics and Informatics, Sofia University "St. Kliment Ohridski",
5 J. Bourchier Blvd, 1164 Sofia, Bulgaria
e-mail: aleksander.a.stefanov@gmail.com

[3]*Institute of Mathematics and Informatics, Bulgarian Academy of Sciences,*
Akad. G. Bonchev St, Bl. 8, 1113 Sofia, Bulgaria

[4]*National Centre of Excellence Mechatronics and Clean Technologies,*
Technical University of Sofia, 8 Kliment Ohridski Blvd, Bl. 8, 1700 Sofia, Bulgaria

[5]*Bulgarian Academy of Sciences, 1, 15 Noemvri St, 1040 Sofia, Bulgaria*